Endopeptidase regulation as a novel function of the Zur-dependent zinc starvation response

Shannon G. Murphy[1, 2], Laura Alvarez[3], Myfanwy C. Adams[4], Shuning Liu[1, 2], Joshua S. Chappie[4], Felipe Cava[3], Tobias Dörr[1, 2]#

[1] Department of Microbiology, Cornell University, Ithaca, New York, USA.

[2] Weill Institute for Cell and Molecular Biology, Cornell University, Ithaca, New York, USA.

[3] Laboratory for Molecular Infection Medicine, Department of Molecular Biology, Umeå University, Umeå, Sweden.

[4] Department of Molecular Medicine, College of Veterinary Medicine, Cornell University, Ithaca, NY, USA.

Running Head: Endopeptidase regulation via zinc starvation response

#Address correspondence to Tobias Dörr, tdoerr@cornell.edu.

Abstract

The cell wall is a strong, yet flexible, meshwork of peptidoglycan (PG) that gives a bacterium structural integrity. To accommodate a growing cell, the wall is remodeled by both PG synthesis and degradation. *Vibrio cholerae* encodes a group of three nearly identical zinc-dependent endopeptidases (EPs) that hydrolyze PG to facilitate cell growth. Two of these (*shyA* and *shyC*) are housekeeping genes and form a synthetic lethal pair, while the third (*shyB*) is not expressed under standard laboratory conditions. To investigate the role of ShyB, we conducted a transposon screen to identify mutations that activate *shyB* transcription. We found that *shyB* is induced as part of the Zur-mediated zinc starvation response, a mode of regulation not previously reported for cell wall lytic enzymes. *In vivo*, ShyB alone was

sufficient to sustain cell growth in low-zinc environments. *In vitro*, ShyB retained its D,D-endopeptidase activity against purified sacculi in the presence of the metal chelator EDTA at a concentration that inhibits ShyA and ShyC. This suggests that ShyB can substitute for the other EPs during zinc starvation, a condition that pathogens encounter while infecting a human host. Our survey of transcriptomic data from diverse bacteria identified other candidate Zur-regulated endopeptidases, suggesting that this adaptation to zinc starvation is conserved in other Gram-negative bacteria.

Importance

The human host sequesters zinc and other essential metals in order to restrict growth of potentially harmful bacteria. In response, invading bacteria express a set of genes enabling them to cope with zinc starvation. In *Vibrio cholerae*, the causative agent of the diarrheal disease cholera, we have identified a novel member of this zinc starvation response: a cell wall hydrolase that retains function in low-zinc environments and is conditionally essential for cell growth. Other human pathogens contain homologs that appear to be under similar regulatory control. These findings are significant because they represent, to our knowledge, the first evidence that zinc homeostasis influences cell wall turnover. Anti-infective therapies commonly target the bacterial cell wall and, therefore, an improved understanding of how the cell wall adapts to host-induced zinc starvation could lead to new antibiotic development. Such therapeutic interventions are required to combat the rising threat of drug resistant infections.

Introduction

The cell wall provides a bacterium with structural integrity and serves as a protective layer guarding against a wide range of environmental insults. Due to its importance for bacterial survival, the cell wall is a powerful and long-standing target for antibiotics (1). The wall is composed primarily of peptidoglycan (PG), a polymer of β-(1,4) linked N-acetylglucosamine (NAG) and N-acetylmuramic acid (NAM) sugar strands (2) (**Fig. 1A**). NAM peptide side chains are cross-linked to peptides on adjacent

51 strands, enabling the PG to assemble into a meshlike structure called the sacculus (3). In Gram-negative
52 bacteria, the sacculus is a single PG layer that is sandwiched between an inner and an outer membrane
53 (4). This thin wall must be rigid enough to maintain cell shape and to contain high intracellular pressures
54 (3, 5). However, the wall must also be flexible enough to accommodate cell elongation, cell division,
55 and the insertion of *trans*-envelope protein complexes (6). This requirement for both rigidity and
56 flexibility necessitates continuous remodeling of the cell wall, which is accomplished by a delicate
57 interplay between PG synthesis and degradation. Inhibition or dysregulation of process can cause growth
58 cessation or cell lysis, rendering the mechanisms of cell wall turnover an attractive target for new
59 antibiotic development (7, 8).

60 PG synthesis is mediated by Penicillin Binding Proteins (PBPs, the targets for beta-lactam
61 antibiotics) and SEDS proteins (9). These proteins collectively catalyze cell wall synthesis through two
62 main reactions: transglycosylation (TG) to elongate the sugar backbone and transpeptidation (TP) to
63 crosslink the peptide stems of adjacent strands (2). Cell wall turnover is mediated by "autolysins", a
64 collective term for diverse and often redundant enzymes (amidases, carboxypeptidases, lytic
65 transglycosylases and endopeptidases) that are able to cleave PG at almost any chemical bond (6).
66 Endopeptidases (EPs), for example, hydrolyze the peptide crosslinks that covalently link adjacent PG
67 strands, effectively reversing the TP reaction. EPs are crucial for cell elongation in both Gram-positive
68 and Gram-negative rod-shaped bacteria (10-12), presumably because they create gaps in the PG
69 meshwork to allow for the insertion of new cell wall material. Consistent with this proposed role, EP
70 overexpression promotes aPBP activity in *Escherichia coli*, likely through the generation of initiation
71 sites for PG synthesis (13).

72 While EPs are essential for growth, they are also main drivers of PG degradation after inhibition
73 of PBPs (14, 15). Thus, EP activity must be tightly controlled under normal growth conditions. EPs in
74 two divergent bacterial species (*E. coli* and *Pseudomonas aeruginosa*) are proteolytically degraded to
75 adapt to conditions that require changes in PG cleavage activity (16, 17), such as the transition into

76 stationary phase. In *Bacillus subtilis*, EP expression is regulated by growth-phase dependent sigma
77 factors (18-21). However, it is not known how EP expression is modified in response to specific
78 environmental stresses.

79 In this study, we investigate the role of specialized EPs in *V. cholerae*, the causative agent of the
80 diarrheal disease cholera. *V. cholera* encodes three nearly identical EPs that are homologous to the well-
81 characterized D,D-endopeptidase MepM in *E. coli* (10). Each EP contains a LysM domain that likely
82 binds PG (22) and a Zn^{2+}-dependent M23 catalytic domain that hydrolyzes peptide cross links (23) (**Fig.
83 1B**). We previously showed that two of these (ShyA and ShyC) are housekeeping EPs that are
84 collectively essential for growth (12). The gene encoding the third EP, *shyB*, is not transcribed under
85 standard laboratory conditions (LB medium) and thus little is known about its biological function. To
86 elucidate the role of ShyB, we conducted a transposon screen to identify mutations that promote *shyB*
87 expression in LB. We found that *shyB* is induced by zinc starvation and, unlike the other two M23 EPs,
88 ShyB enzymatic activity is resistant to treatment with the metal chelator EDTA. These data suggest that
89 ShyB acts as an alternative EP to ensure proper PG maintenance under zinc limiting conditions.
90 Importantly, this represents the first characterization of an autolysin that is controlled by Zur-mediated
91 zinc homeostasis and provides insight into how other Gram-negative pathogens might adapt to zinc-
92 starvation when colonizing a human host.
93

94 **Results**

95 ***shyB* is repressed in LB, but transcribed in minimal medium.**

96 The hydrolytic activity of autolysins needs to be carefully controlled to maintain cell wall
97 integrity. We therefore considered it likely that specialized autolysins are transcriptionally regulated and
98 only induced when required. To test this, we examined expression patterns of the LysM/M23
99 endopeptidases using *lacZ* transcriptional fusions. We first compared promoter activity on LB and M9
100 agar, as our previous work showed that a Δ*shyB* mutation exacerbates a Δ*shyA* growth defect in M9

101 minimal medium (12). The P_{shyA}*:lacZ* and P_{shyC}*:lacZ* reporters generated a blue colony color on both LB
102 and M9 minimal agar (**Fig. 1C**), meaning that these promoters are actively transcribed on both media.
103 This is consistent with ShyA and ShyC's role as housekeeping EPs (12). In contrast, P_{shyB}*:lacZ* yielded
104 blue colonies on M9 minimal medium only, indicating that the *shyB* promoter is induced in M9 but
105 repressed in LB.
106
107 ***shyB* is induced by zinc starvation.**
108 To elucidate the specific growth conditions that favor *shyB* expression, we sought to identify the
109 genetic factors controlling *shyB* transcription. To this end, we subjected the transcriptional reporter
110 strain to Himar1 mariner transposon mutagenesis and screened for P_{shyB}*:lacZ* induction (blue colonies)
111 on LB agar. After two independent rounds of mutagenesis (50,000 total colonies), the screen yielded 26
112 blue colored insertion mutants. These were divided into two distinct classes according to colony color:
113 12 dark blue and 14 light blue colonies. Strikingly, arbitrary PCR (24) mapped all 26 transposon
114 insertions to two chromosomal loci involved in zinc homeostasis: *vc0378/zur* (dark blue colonies) and
115 *vc2081-2083/znuABC* (light blue colonies) (**Fig. 2A**). Zur is a fur-family transcriptional regulator and
116 the central repressor in the zinc starvation response (25). In zinc-rich conditions, Zur and its Zn^{2+}
117 corepressor bind to promoters containing a "Zur box" and block transcription (26). In low-zinc
118 conditions, Zur dissociates from promoters to induce the zinc starvation response (27). This regulon
119 includes genes encoding zinc uptake systems (i.e. *znuABC, zrgABCDE*) (28) and zinc-independent
120 paralogs that replace proteins that ordinarily require zinc for function (i.e. ribosomal proteins) (29). The
121 Zur-controlled *znuABC* locus encodes *V. cholerae*'s high affinity zinc uptake system (28). To validate
122 the transposon hits, we constructed clean deletions of *zur* and *znuA* in the P_{shyB}*:lacZ* reporter strain.
123 Deletion of either gene resulted in activation of the *shyB* promoter on LB agar, and *shyB* repression was
124 restored by expressing the respective genes *in trans* (**Fig. S1**). Thus, *shyB* is induced under conditions
125 that are expected to either mimic (*zur* inactivation) or impose (*znuA(BC)* inactivation) zinc starvation.

126 If zinc starvation is the factor inducing *shyB* expression in M9, we would expect the P_{shyB}*:lacZ*
127 reporter to be repressed by external zinc addition. Indeed, supplementing M9 with 10 μM of $ZnSO_4$ was
128 sufficient to turn off the *shyB* promoter in a wild-type (WT) background (**Fig. 2B**), whereas repression
129 could not be achieved by adding in other transition metals (iron and manganese) (**Fig. S2**). In a *Δzur*
130 background, the *shyB* promoter remained active even when M9 was supplemented with exogenous zinc
131 (**Fig. 2B**), indicating that Zur is required for P_{shyB} repression. We also found that zinc supplementation
132 somewhat repressed the *shyB* promoter in Δ*znuA*, suggesting that *V. cholerae* can uptake zinc even in
133 the absence of its primary transporter. Indeed, *V. cholerae* encodes a second, lower affinity zinc
134 acquisition system (*zrgABCDE*) to maintain zinc homeostasis (28).
135

136 **Zur directly binds the *shyB* promoter.**

137 Given Zur's well-defined role as a transcriptional regulator (26) and its requirement for P_{shyB} repression
138 in zinc-rich media, we hypothesized that Zur directly binds the *shyB* promoter. To test this, we retrieved
139 a Zur box sequence logo built from 62 known regulatory targets in Vibrionaceae (30, 31) and aligned it
140 with the *shyB* promoter region. This alignment identified a highly conserved Zur box characterized by
141 an inverted, AT-rich repeat (**Fig. 3A**). We used 5'-RACE to locate the *shyB* transcriptional start site (tss)
142 and found that the putative Zur box overlaps both the -10 region and tss. A bound Zur/Zn^{2+} complex at
143 this position likely prevents RNA polymerase binding and thereby prevents transcription (32).

144 To determine if Zur binds the *shyB* promoter *in vitro*, we incubated purified Zur with a labeled
145 DNA probe encoding the P_{shyB} Zur box. Binding was assessed in the presence of $ZnCl_2$ using an
146 electrophoretic mobility shift assay (EMSA). As evident by a band shift, Zur formed a complex with the
147 P_{shyB} DNA *in vitro* (**Fig. 3B, Lanes 1-2**). To examine DNA binding specificity, a 100-fold molar excess
148 of unlabeled specific (S) or non-specific (NS) competitor DNA was included in the binding reaction.
149 The S competitor, which carries an identical sequence as the labeled probe, effectively sequestered Zur
150 and increased the amount of unbound, labeled probe (**Lane 3**). Meanwhile, the NS competitor was

151 ineffective at binding Zur (**Lane 4**). These data indicate that the *shyB* promoter contains an authentic
152 Zur box and we conclude that *shyB* is a novel member of the Zur regulon.
153
154 **ShyB supports growth in chelated medium.**
155 As *shyB* is part of the Zur-mediated zinc starvation response, we hypothesized that ShyB endopeptidase
156 activity supports cell growth when zinc availability is low. To induce zinc starvation and robustly
157 derepress the Zur regulon, *V. cholerae* strains were grown in M9 minimal medium supplemented with
158 TPEN (N,N,N′,N′-Tetrakis(2-pyridylmethyl)ethylenediamine), an intracellular metal chelator with high
159 affinity for zinc (33). As expected from our genetic analysis, TPEN addition resulted in the production
160 of ShyB protein, which could be reversed by adding zinc (**Fig. S3**).
161 We first tested whether native *shyB* could restore Δ*shyAC* growth under zinc-starvation
162 conditions. *shyA* and *shyC* deletions were generated in a parent strain expressing an IPTG-inducible
163 copy of *shy*A (*lacZ*::P_{tac}:*shyA),* as these genes are conditionally essential in rich media (12). In the
164 absence of IPTG, we found that chelation with either TPEN or EDTA (a more general divalent metal ion
165 chelator), induced growth of Δ*shyAC*, but not in the mutant that additionally lacked *shyB* (**Fig. 4A**; **Fig.**
166 **S4**). As expected, chelation-dependent growth of Δ*shyAC* could be suppressed by adding zinc (**Fig. 4B**;
167 **Fig. S4**). These data suggest that induction of *shyB* alone is sufficient to sustain *V. cholerae* growth, and
168 synthetic lethality of *shyA* and *shyC* is due to the lack of *shyB* expression under laboratory growth
169 conditions. Consistent with this interpretation, we were able to generate a Δ*shyAC* knockout in a Δ*zur*
170 background (**Fig. S5**) or in a strain exogenously overexpressing *shyB* (**Fig. S6**).
171 A Δ*shyB* mutant alone did not exhibit a significant growth defect in M9 TPEN (**Fig. 4C**);
172 however, autolysins often need to be deleted in combination to elicit a substantial phenotype (11). We
173 therefore generated all possible combinations of LysM/M23 endopeptidase deletions to broadly dissect
174 the relevance of zinc concentrations for EP activity. Of these, the Δ*shyAB* double mutant failed to grow
175 in the presence of TPEN (**Fig. 4C**). This indicates that ShyC, the only essential LysM/M23 EP in the

176 Δ*shyAB* mutant, cannot support growth in zinc-starved media. In contrast, only the Δ*shyAC* mutant
177 failed to grow in zinc-replete medium and this can be explained by Zur-mediated *shyB* repression (**Fig.**
178 **4D**). This tradeoff in synthetic lethality partners tentatively suggests that ShyB may function as a
179 replacement for ShyC during zinc starvation. ShyC protein levels, as measured by Western Blot, were
180 not reduced in the presence of TPEN, ruling out the possibility that Δ*shyAB* lethality reflects
181 transcriptional downregulation or degradation of ShyC (**Fig S3**). Rather, these observations suggest that
182 ShyC activity is more sensitive to zinc-chelation than the other EPs. Alternatively, TPEN might induce
183 changes in PG architecture that make it resistant to cleavage by ShyC.
184

185 **ShyB is an EDTA-resistant D,D-endopeptidase *in vitro*.**

186 ShyB is predicted to be a D,D-endopeptidase but biochemical evidence is lacking. Thus, we measured
187 the *in vitro* hydrolytic activity of each EP against *V. cholerae* sacculi. Each protein was recombinantly
188 purified without the hydrophobic signal sequence or transmembrane domain ($ShyA_{\Delta 1\text{-}35}$, $ShyB_{\Delta 1\text{-}34}$, and
189 $ShyC_{\Delta 1\text{-}33}$) to increase stability *in vitro*. As a negative control, we purified ShyB with a mutation
190 (H370A) in the active site that is expected to abolish activity. EPs were incubated with purified sacculi
191 (see Methods for details) and the soluble PG fragments released by digestion were separated using high
192 pressure liquid chromatography (HPLC) and quantified by spectrophotometry. As predicted, all three
193 enzymes, but not the H370A mutant, hydrolyzed *V. cholerae* sacculi and generated soluble PG
194 fragments (**Fig. 5A**; **Fig. S7**). Sacculi digestion with ShyA and ShyC resulted in a similar profile of PG
195 fragments, indicating similar hydrolytic activity *in vitro*. In contrast, the ShyB chromatogram showed
196 more peaks with shorter retention times. These observations suggest that ShyB further processes the
197 sacculi into smaller fragments. Consistent with this, ShyB was able to further process PG pre-digested
198 with ShyA or ShyC, while these EPs only slightly modified ShyB-digested PG (**Fig. S8**). To determine
199 which muropeptides remain in the insoluble pellet after EP digestion, muramidase was used to digest the
200 PG sugar backbone (β 1→4 linkages). The resulting soluble products produced a single peak,

201 corresponding to a M4 monomer. This indicates that all three LysM/M23 EPs exhibit D,D-
202 endopeptidase activity *in vitro* (**Fig. 5B**).
203 M23 domains require a coordinated zinc ion to carry out PG hydrolysis (23). However, based on
204 its regulation by Zur, we hypothesized that ShyB evolved to function in zinc-limited environments. To
205 test this, we repeated the *in vitro* PG hydrolysis assays under metal-limited conditions by using the
206 divalent cation chelator EDTA. Strikingly, ShyB retained its activity in the presence of EDTA (1 mM),
207 while ShyA and ShyC activity was completely abolished (**Fig. 5C-D**). This is consistent with results
208 previously obtained for ShyA (12). These data suggest that ShyB has a high affinity for, or can function
209 without, divalent cations like zinc.
210
211 **ShyB localizes to the division septum.**
212 Endopeptidases often differ in their cellular localization and this is an important determinant of EP
213 function *in vivo* (34). We previously reported that ShyA, a sidewall hydrolase, remains diffuse
214 throughout the periplasm, while ShyC localizes to the septum (midcell) during division (12). To
215 investigate the relative role of ShyB, we constructed a functional ShyBmsfGFP translational fusion (**Fig.**
216 **S9**) and visualized its localization using epifluorescence microscopy. ShyBmsfGFP strongly localized to
217 the septum as cells prepared to divide. (**Fig. 6**). Septal localization suggests that ShyB and ShyC are
218 involved in cell division. However, neither the Δ*shyB* nor Δ*shyC* mutant, either alone or in combination,
219 have a division defect and we thus do not know the significance of endopeptidase activity at the septum
220 in *V. cholerae.*
221
222 **Zur-controlled endopeptidases are widespread in divergent bacteria.**
223 Zur-controlled EPs appear to be widespread in *Vibrionaceae*. Using BLAST homology searches, we
224 have identified isolates from 30 different non-cholera *Vibrio* species that contain a ShyB homolog with a
225 Zur box upstream of the gene encoding it (**Table S1**) (35). To assess the significance of zinc

226 homeostasis for EP regulation more broadly, we surveyed published microarray and RNAseq datasets
227 from diverse bacteria for differential EP expression (36-45). *Yersinia pestis* CO92, the causative agent of
228 plague, encodes a ShyB/MepM homolog (YPO2062) that is significantly up-regulated in a *Δzur* mutant
229 (36). YPO2062 does not contain its own Zur box, but is adjacent to *znuA* and may thus be co-transcribed
230 as part of the same operon (**Fig. 7**). Similarly, *mepM* (b1856) is located adjacent to the *znu* operon in
231 laboratory (K12 MG1655) and pathogenic *E. coli* (Enterohemorrhagic O157:H7 and Enteropathogenic
232 O127:H6). Two independent microarray studies in *E. coli*, one of which was validated by qPCR, showed
233 that this EP was transcriptionally upregulated in response to zinc starvation (44, 45). These data suggest
234 that MepM and its homologs are Zur-regulated EPs. Notably, this *znu*/EP arrangement is conserved in
235 many other Gram-negative pathogens, including *Salmonella typhimurium* (STM1890), *Enterobacter*
236 *cloacae* (ECL_0-1442), and *Klebsiella pneumoniae* (KPK_1913). Lastly, *A. baumannii*, an important
237 nosocomial pathogen, possesses two M23 endopeptidases differentially transcribed in a *Δzur* mutant.
238 A1S_3329 is up-regulated and A1S_0820 is down-regulated compared to a wild-type strain (37),
239 suggesting that these EPs are also under zinc starvation control. Collectively, these data suggest that zinc
240 homeostasis and cell wall turnover are linked in a wide array of Gram-negative bacteria.
241

242 **Discussion**

243 **Highly redundant endopeptidases support cell growth.**

244 Endopeptidase activity is essential for cell growth in both Gram-negative and Gram-positive bacteria,
245 supporting the long-standing hypothesis that autolysins create space in the PG meshwork for the
246 insertion of new cell wall material (8). As with other autolysins, EPs are highly redundant but exhibit
247 slight differences in cellular localization (i.e. septal or sidewall) (12, 20, 46), substrate specificity (10,
248 47) and relative abundance during each growth phase (11, 46). Our previous work in *V. cholerae*
249 identified three LysM/M23 zinc metallo-endopeptidases: two (ShyA and ShyC) are housekeeping
250 enzymes that are conditionally essential for growth, while the third (ShyB) is not expressed under

251 standard laboratory conditions (12). In this study, we define *shyB* as a new member of the Zur regulon
252 and demonstrate that ShyB can replace the other EPs *in vivo* when zinc concentrations are limiting. This
253 is a novel mechanism for regulating autolysins and establishes a link between two essential processes:
254 cell wall turnover and metal ion homeostasis.
255
256 **Zinc availability affects the expression and activity of cell wall hydrolases.**
257 Zur represses *shyB* transcription in zinc-rich growth conditions. This is consistent with our initial
258 observation that the *shyB* promoter is active on M9 and repressed on LB agar. These respective media
259 differ markedly in terms of zinc content; M9 contains no added zinc while LB naturally contains high
260 levels of zinc ions (~12.2 μM) (48). We found that adding zinc (10 μM) to M9 represses the *shyB*
261 promoter and hence the zinc starvation response. As a cautionary note, this suggests that *V. cholerae* is
262 starved for zinc in M9, a complication not usually considered when interpreting results obtained in this
263 medium.
264 Based on its membership in the Zur regulon, it is likely that ShyB evolved to function in low-
265 zinc environments. Indeed, ShyB endopeptidase activity is resistant to high EDTA concentrations *in*
266 *vitro*. In an apparent contradiction, the ShyB crystal structure models a zinc ion in the active site (49). It
267 is possible that ShyB has a higher affinity for zinc than the other EPs, but we cannot yet exclude the
268 possibility that ShyB utilizes other metal cofactors. ShyA appears to have an intermediate ability to
269 function in low zinc environments; we found that ShyA can support cell growth in the absence of the
270 other two EPs in TPEN-treated medium (like ShyB), yet EDTA inhibited its activity *in vitro*. This
271 observation is likely a consequence of the high EDTA concentrations (1 mM) used in the biochemical
272 assays, which do not permit wild type *V. cholerae* growth. The ability to sustain growth in the presence
273 of TPEN, however, indicates that ShyA function is less affected by metal starvation than ShyC.
274 Since ShyA functions in chelated medium, we tentatively hypothesize that *shyB* is derepressed to
275 compensate for a loss of ShyC activity. This model is supported by localization data and ShyC's

276 sensitivity to chelating conditions, both *in vivo* and *in vitro*, that induce *shyB* expression. We did not
277 observe any defects in Δ*shyB*, Δ*shyC,* or Δ*shyBC* mutants; however, septal EP deletion causes division
278 defects (i.e. filamentation) in other bacteria (20) . It is thus possible that the role of septal EPs in *V.*
279 *cholerae* is more prominent under conditions not yet assayed. In our experiments, diffuse ShyA might
280 be present at sufficient concentrations at the septum to alleviate any obvious division defects.
281

282 **Bacteria encounter zinc starvation while infecting a host.**

283 Proteins that retain function in low-zinc conditions likely play important roles in pathogenesis as
284 bacteria encounter zinc-starvation inside the human host (50). Vertebrates and other organisms sequester
285 metals to restrict the growth of potentially harmful bacterial, a defense strategy referred to as "nutritional
286 immunity" (50). In response, bacteria employ zinc-starvation responses to maintain essential cellular
287 processes (51). Zinc importers (*znuABC* and *zrgABCDE*), for example, are critical for host colonization
288 and infection in *V. cholerae* (28), *A. baumannii* (52), pathogenic *E. coli* (53, 54), *Salmonella enterica*
289 (55), and others (56). It is tempting to speculate that ShyB, a rather unusual addition to the Zur regulon,
290 supports PG remodeling in a zinc-depleted host environment. Consistent with this idea**,** *shyB* is located
291 on a mobile genomic island (VSP-II) that is strongly associated with the current (seventh) Cholera
292 pandemic (57). The current pandemic strain emerged in the 1960's and, owing to its higher spread
293 capability, replaced its pandemic predecessors (58). This suggests that VSP-II (and thus possibly ShyB)
294 conferred a fitness advantage to pathogenic *V. cholerae*.

295 Importantly, Zur-controlled M23 endopeptidases do not appear to be confined to *V. cholerae*.
296 Diverse bacteria, including notable human pathogens, possess a conserved *shyB*/*mepM*/*yebA* homolog
297 adjacent to the Zur-controlled *znu* operon. Transcriptomic data from both *Y. pestis* and *E. coli* support
298 the prediction that this EP is upregulated along with the zinc importer. The conservation of zinc-
299 regulated EPs in divergent Gram-negative pathogens suggests that there may be a widely conserved
300 mechanism for maintaining cell wall homeostasis in low zinc environments. Importantly, this may

301 confer an important adaptation to host-induced zinc starvation. These findings in *V. cholerae* will inform
302 future investigations examining the interplay between cell wall turnover and zinc homeostasis.
303

304 **Experimental Procedures**

305 **Bacterial growth conditions.**

306 Cells were grown by shaking (200 rpm) at 37°C in 5 mL of LB medium unless otherwise indicated. M9
307 minimal medium with glucose (0.4%) was prepared with ultrapure Mili-Q water to minimize zinc
308 contamination. When appropriate, antibiotics were used at the following concentrations: streptomycin
309 (200 µg mL^{-1}), ampicillin (100 µg mL^{-1}), and kanamycin (50 µg mL^{-1}). IPTG (200 µM) was added to all
310 liquid and solid media if required to sustain *V. cholerae* growth. X-gal (40 µg mL^{-1}) was added to plates
311 for blue-white screening.
312

313 **Plasmid and strain construction.**

314 All genes were PCR amplified from *V. cholerae* El Tor N16961 genomic DNA. Plasmids were built
315 using isothermal assembly (59) with the oligonucleotides summarized in **Table S2**. The suicide vector
316 pCVD442 was used to make gene deletions via homologous recombination (60); 700 bp regions
317 flanking the gene of interest were amplified for Δ*zur* (SM89/90 + SM91/92), Δ*znuA* (SM107/108 +
318 SM109/110), and Δ*znuABC* (SM93/94, SM95/96) and assembled into XbaI digested pCVD442.
319 Endopeptidase deletion constructs were built as described previously (12). Chromosomal delivery
320 vectors (pJL-1 and pTD101) were used to insert genes via double cross-over into native *lacZ*. To
321 construct the *shyB* transcriptional reporter, 500 bp upstream of *shyB* were amplified (SM1/2) and
322 assembled into NheI-digested pAM325 to yield a P_{shyB}:*lacZ* fusion. This fusion was amplified (SM3/4)
323 and cloned into StuI-digested pJL-1 (61). To complement gene deletions, *zur* (SM99/100) and *znuA*
324 (SM113/114) were cloned into SmaI-digested pBAD: a chloramphenicol resistant, arabinose-inducible
325 plasmid. To construct the ShyBmsfGFP C-terminal translational fusion, *shyB* (SM181/63) and *msfGFP*

326 (SM65/66) were amplified with an overhang encoding a 10 amino acid flexible linker
327 (gctggctccgctgctggttctggcgaattc). These fragments were assembled into SmaI-digested pTD101, which
328 positions the fusion under an IPTG-inducible promoter. In a similar manner, pTD101(*shyB*) was
329 constructed with SM181/182 and pTD100(*shyA*) was built as previously described (12). An additional
330 chromosomal delivery vector (pSGM100) was built for crossover into VC0817. *shyB* (SM141/SM55)
331 was placed under arabinose-inducible control by cloning into SmaI-digested pSGM100. All assemblies
332 were initially transformed into *E. coli* DH5α λpir and then into SM10 λpir for conjugation into *V.*
333 *cholerae.*

334 All strains are derivatives of *V. cholerae* El Tor N16961 (WT). To conjugate plasmids into *V.*
335 *cholerae*, SM10 λpir donor strains carrying pCVD442, pTD101, PJL-1, or pSGM100 plasmids were
336 grown in LB/ampicillin. Recipient *V. cholerae* strains were grown overnight in LB/streptomycin.
337 Stationary phase cells were pelleted by centrifugation (6,500 rpm for 3 min) and washed with fresh LB
338 to remove antibiotics. Equal ratios of donor and recipient (100µL:100 µL) were mixed and spotted onto
339 LB agar plates. After a 4-hour incubation at 37°C, cells were streaked onto LB containing streptomycin
340 and ampicillin to select for cross-over recipients. Colonies were purified and cured through two rounds
341 of purification on salt free sucrose (10%) agar with streptomycin. Insertions into native *lacZ* (via pJL-1,
342 pTD101) were identified by blue-white colony screening on X-gal plates. Gene deletions (via
343 pCVD442) were checked via PCR screening with the following primers: Δ*shyA* (TD503/504), Δ*shyB*
344 (SM30/31), Δ*shyC* (TD701/702), Δ*zur* (SM122/123), Δ*znuA* (SM119/120), and Δ*znuABC* (SM119/121).
345

346 **Transposon mutagenesis and arbitrary PCR.**

347 The *shyB* transcriptional reporter was mutagenized with Himar1 mariner transposons, which were
348 delivered via conjugation by an SM10 λpir donor strain carrying pSC189 (62). The recipient and donor
349 were grown overnight in LB/streptomycin and LB/ampicillin, respectively. Stationary phase cells were
350 pelleted by centrifugation (6,500 rpm for 3 min) and washed with fresh LB to remove antibiotics. Equal

351 ratios of donor and recipient (500 µL:500 µL) were mixed and spotted onto 0.45 µm filter disks adhered
352 to pre-warmed LB plates. After a 4-hour incubation at 37°C, cells were harvested by aseptically
353 transferring the filter disks into conical tubes and vortexing in fresh LB. The cells were spread onto LB
354 agar containing streptomycin to kill the donor strain, kanamycin to select for transposon mutants, and X-
355 gal to allow for blue-white colony screening. Plates were incubated at 30°C overnight followed by two
356 days at room temperature. To identify the transposon insertion site, purified colonies were lysed via
357 boiling and used directly as a DNA template for arbitrary PCR. As described elsewhere**,** this technique
358 amplifies the DNA sequence adjacent to the transposon insertion site through successive rounds of PCR
359 (24). Amplicons were Sanger sequenced and high quality sequencing regions were aligned to the
360 *N16961* genome using BLAST (35).
361
362 **5' rapid amplification of cDNA ends.**
363 The *shyB* transcription start site was identified with 5' rapid amplification of cDNA ends (5' RACE). To
364 obtain a *shyB* transcript, *Δzur* was grown in LB at 37°C until cells reached mid-exponential phase
365 (OD_{600} = 0.5) and RNA was extracted using Trizol and acid:phenol chloroform (Ambion). DNA
366 contamination was removed through two RQ1 DNase (Promega) treatments and additional acid:phenol
367 chloroform extractions. cDNA synthesis was performed with MultiScribe reverse transcriptase
368 (ThermoFisher) and a *shyB* specific primer (SM270). cDNA was column purified and treated with
369 terminal transferase (New England BioLabs) to add a homopolymeric cytosine tail to the 3' end. The
370 cDNA was amplified through two rounds of touchdown PCR with a second gene-specific primer
371 (SM271) and the Anchored Abridged Primer (ThermoFisher). The PCR product was Sanger sequenced
372 using primer SM271.
373
374 **Electrophoretic mobility shift assay.**

375 The LightShift Chemiluminescent EMSA kit (ThermoFisher) was used to detect Zur-promoter binding.
376 41 bp complimentary oligos (SM264/265) containing the putative *shyB* Zur box, with and without a 5'
377 biotin label, were annealed according to commercial instructions (Integrated DNA Technologies). 20 µL
378 binding reactions contained buffer, Poly dI-dC (50 ng μL^{-1}), $ZnCl_2$ (5 µM), labeled probe (1 pmol), and
379 purified Zur (600 nM). Unlabeled specific or non-specific competitor oligos were added in 100-fold
380 molar excess. Reactions were incubated on ice for 1 hour, electrophoresed on a 6% DNA retardation gel
381 (100 V, 40 min), and wet transferred to a Biodyne B membrane (100 V, 30 min) (ThermoFisher) in a
382 cold room. The membrane was developed using chemiluminescence according to the manufacturer's
383 instructions and imaged using a Bio-Rad ChemiDoc MP imaging system.
384

385 **Protein expression and purification.**

386 DNA encoding N-terminally truncated LysM/M23 endopeptidases ($ShyA_{\Delta 1\text{-}35}$, $ShyB_{\Delta 1\text{-}34}$, and $ShyC_{\Delta 1\text{-}33}$)
387 and full length Zur was PCR amplified from genomic DNA, while template for the ShyB H370A
388 mutation was commercially synthesized (Integrated DNA Technologies). Shy constructs were cloned
389 into pCAV4, and Zur into pCAV6, both modified T7 expression vectors that introduce an N-terminal
390 6xHis-NusA tag (pCAV4) or 6xHis-MBP tag (pCAV6) followed by a Hrv3C protease site upstream of
391 the inserted sequence. Constructs were transformed into BL21(DE3) cells, grown at 37°C in Terrific
392 Broth supplemented with carbenicillin (100 mg mL^{-1}) to an OD_{600} of 0.8-1.0, and then induced with
393 IPTG (0.3 mM) overnight at 19°C. $ZnCl_2$ (50 µM) was added during Zur induction. Cells were
394 harvested via centrifugation, washed with nickel loading buffer (NLB) (20 mM HEPES pH 7.5, 500 mM
395 NaCl, 30 mM imidazole, 5% glycerol (v:v), 5 mM β –Mercaptoethanol), pelleted in 500mL aliquots, and
396 stored at -80°C.

397 Pellets were thawed at 37°C and resuspended in NLB supplemented with PMSF (10 mM),
398 DNAse (5 mg), $MgCl_2$ (5 mM), lysozyme (10 mg mL^{-1}), and one tenth of a complete protease inhibitor
399 cocktail tablet (Roche). All buffers used in Zur purification were supplemented with $ZnCl_2$ (1 µM). Cell

400 suspensions were rotated at 4°C, lysed via sonication, centrifuged, and the supernatant was syringe
401 filtered using a 0.45 µM filter. Clarified samples were loaded onto a $NiSO_4$ charged 5 mL HiTrap
402 chelating column (GE Life Sciences), and eluted using an imidazole gradient from 30 mM to 1M.
403 Hrv3C protease was added to the pooled fractions and dialyzed overnight into cation exchange loading
404 buffer (20 mM HEPES pH 7.5, 50 mM NaCl, 1 mM EDTA, 5% glycerol (v:v), 1 mM DTT). Cleaved
405 Shy proteins were loaded onto a 5 mL HiTrap SP HP column and cleaved Zur was loaded onto a 5mL
406 HiTrap Heparin HP column (GE Life Sciences). All constructs were eluted along a NaCl gradient from
407 50mM to 1M. Fractions were concentrated and injected onto a Superdex 75 16/600 equilibrated in Size
408 Exclusion Chromotography buffer (20 mM HEPES pH7.5, 150 mM KCl, 1 mM DTT). Zur dimers
409 coeluted with MBP on the sizing column and were subsequently incubated with amylose resin (New
410 England BioLabs) at 4°C and Zur was collected from a gravity column. Final purified protein
411 concentrations were determined by SDS-PAGE and densitometry compared against BSA standards:
412 ShyA, 5.72 mg mL^{-1}; ShyB, 5.72 mg mL^{-1}; ShyB H320A, 2.35 mg mL^{-1}; ShyC, 17.93 mg mL^{-1}; Zur,
413 0.31 mg mL^{-1}.
414
415 **Sacculi digestion assay.**
416 Peptidoglycan from stationary phase *V. cholerae* cells was extracted and purified via SDS boiling and
417 muramidase digestion (63). 10 µL of sacculi and 10 µg of enzyme were mixed in 50 µL buffered
418 solution (50 mM Tris-HCl pH 7.5, 100 mM NaCl) in the absence or presence of 1 mM EDTA.
419 Digestions were incubated for 16 h at 37°C. Soluble products were harvested and the remaining pellet
420 was further digested with muramidase. All soluble products were reduced with sodium borohydride,
421 their pH adjusted, and injected into a Waters UPLC system (Waters, Massachusetts, USA) equipped
422 with an ACQUITY UPLC BEH C18 Column, 130 Å, 1.7 µm, 2.1 mm × 150 mm (Waters) and a dual
423 wavelength absorbance detector. Eluted fragments were separated at 45°C using a linear gradient from

424 buffer A [formic acid 0.1% (v/v)] to buffer B [formic acid 0.1% (v/v), acetonitrile 40% (v/v)] in a 12
425 min run with a 0.175 ml min^{-1} flow, and detected at 204 nm.
426
427 **Growth curve analysis.**
428 Strains were grown overnight in LB/streptomycin with IPTG. Cells were washed in 1X phosphate
429 buffered solution (PBS) and subcultured 1:10 into M9 glucose plus IPTG. After 2 hours shaking at $37^{o}C$,
430 cells were washed and subcultured 1:100 into M9 glucose containing combinations of TPEN (250 nM),
431 ZNSO4 (1 μM), and IPTG (200 μM). The growth of each 200 μL culture in a 100-well plate was
432 monitored by optical density (OD_{600}) on a Bioscreen C plate reader (Growth Curves America).
433
434 **Microscopy and image analysis.**
435 Cells were imaged on an agarose patch (0.8% agarose in M9 minimal medium) using a Leica DMi8
436 inverted microscope. To image the ShyBmsfGFP fusion, cells were exposed to 490 nm for 300 ms.
437 Image analysis, including cell selection and subpixel quantification of fluorescent signal as a function
438 distance from the midcell, was performed in Oufti (64).
439
440 **Acknowledgements**
441 We thank all the members of the Doerr and Chappie Labs for helpful discussions and assistance with
442 this work. We thank members of the John Helmann Lab for lending their expertise and reagents. We
443 thank the faculty, staff, and students at the Weill Institute for Cell and Molecular Biology (WICMB) for
444 their support. Research in the Doerr Lab is supported by start-up funds from Cornell University.
445 Research in the Chappie Lab is supported by the National Institute of Health (NIH). Research in the
446 Cava lab is supported by MIMS, the Knut and Alice Wallenberg Foundation (KAW), the Swedish
447 Research Council and the Kempe Foundation.
448

449

450 **References**

451 1. **Schneider T**, **Sahl H-G**. 2010. An oldie but a goodie – cell wall biosynthesis as antibiotic target
452 pathway. Int J Med Microbiol **300**:161–169.

453 2. **Typas A**, **Banzhaf M**, **Gross CA**, **Vollmer W**. 2012. From the regulation of peptidoglycan
454 synthesis to bacterial growth and morphology. Nat Rev Microbiol **10**:123–136.

455 3. **Höltje JV**. 1998. Growth of the stress-bearing and shape-maintaining murein sacculus of
456 *Escherichia coli*. Microbiol Mol Biol Rev **62**:181–203.

457 4. **Silhavy TJ**, **Kahne D**, **Walker S**. 2010. The bacterial cell envelope. Cold Spring Harb Perspect
458 Biol **2**:a000414.

459 5. **Cabeen MT**, **Jacobs-Wagner C**. 2005. Bacterial cell shape. Nat Rev Microbiol **3**:601–610.

460 6. **Vollmer W**, **Joris B**, **Charlier P**, **Foster S**. 2008. Bacterial peptidoglycan (murein) hydrolases.
461 FEMS Microbiol Rev **32**:259–286.

462 7. **Tomasz A**. 1979. The mechanism of the irreversible antimicrobial effects of penicillins: how the
463 beta-lactam antibiotics kill and lyse bacteria. Annu Rev Microbiol **33**:113–137.

464 8. **Vollmer W**. 2012. Bacterial growth does require peptidoglycan hydrolases. Mol Microbiol
465 **86**:1031–1035.

466 9. **Cho H**, **Wivagg CN**, **Kapoor M**, **Barry Z**, **Rohs PDA**, **Suh H**, **Marto JA**, **Garner EC**,
467 **Bernhardt TG**. 2016. Bacterial cell wall biogenesis is mediated by SEDS and PBP polymerase
468 families functioning semi-autonomously. Nature Microbiology 2016 1:10 **1**:16172.

469 10. **Singh SK**, **SaiSree L**, **Amrutha RN**, **Reddy M**. 2012. Three redundant murein endopeptidases
470 catalyse an essential cleavage step in peptidoglycan synthesis of *Escherichia coli* K12. Mol
471 Microbiol **86**:1036–1051.

472 11. **Hashimoto M**, **Ooiwa S**, **Sekiguchi J**. 2011. The synthetic lethality of lytE cwlO in *Bacillus*
473 *subtilis* is caused by lack of d,l-endopeptidase activity at the lateral cell wall. J Bacteriol **194**:796–
474 803.

475 12. **Dörr T**, **Cava F**, **Lam H**, **Davis BM**, **Waldor MK**. 2013. Substrate specificity of an elongation-
476 specific peptidoglycan endopeptidase and its implications for cell wall architecture and growth of
477 Vibrio cholerae. Mol Microbiol **89**:949–962.

478 13. **Lai GC**, **Cho H**, **Bernhardt TG**. 2017. The mecillinam resistome reveals a role for
479 peptidoglycan endopeptidases in stimulating cell wall synthesis in *Escherichia coli*. PLoS Genet
480 **13**:e1006934.

481 14. **Dörr T**, **Davis BM**, **Waldor MK**. 2015. Endopeptidase-Mediated Beta Lactam Tolerance. PLoS
482 Pathog **11**:e1004850.

483 15. **Kitano K**, **Tuomanen E**, **Tomasz A**. 1986. Transglycosylase and endopeptidase participate in
484 the degradation of murein during autolysis of *Escherichia coli*. J Bacteriol **167**:759–765.

485 16. **Singh SK**, **Parveen S**, **SaiSree L**, **Reddy M**. 2015. Regulated proteolysis of a cross-link–specific
486 peptidoglycan hydrolase contributes to bacterial morphogenesis. Proc Natl Acad Sci USA
487 **112**:10956–10961.

488 17. **Srivastava D**, **Seo J**, **Rimal B**, **Kim SJ**, **Zhen S**, **Darwin AJ**. 2018. A Proteolytic Complex
489 Targets Multiple Cell Wall Hydrolases in *Pseudomonas aeruginosa*. mBio **9**:e00972–18.

490 18. **Britton RA**, **Eichenberger P**, **Gonzalez-Pastor JE**, **Fawcett P**, **Monson R**, **Losick R**,
491 **Grossman AD**. 2002. Genome-wide analysis of the stationary-phase Sigma factor (Sigma-H)
492 Regulon of *Bacillus subtilis*. J Bacteriol **184**:4881–4890.

493 19. **Ishikawa S**, **Hara Y**, **Ohnishi R**, **Sekiguchi J**. 1998. Regulation of a new cell wall hydrolase
494 gene, cwlF, which affects cell separation in *Bacillus subtilis*. J Bacteriol **180**:2549–2555.

495 20. **Ohnishi R**, **Ishikawa S**, **Sekiguchi J**. 1999. Peptidoglycan hydrolase LytF plays a role in cell
496 separation with CwlF during vegetative growth of *Bacillus subtilis*. J Bacteriol **181**:3178–3184.

497 21. **Yamaguchi H**, **Furuhata K**, **Fukushima T**, **Yamamoto H**, **Sekiguchi J**. 2004. Characterization
498 of a new *Bacillus subtilis* peptidoglycan hydrolase gene, yvcE (named cwlO), and the enzymatic
499 properties of its encoded protein. J Biosci Bioeng **98**:174–181.

500 22. **Buist G**, **Steen A**, **Kok J**, **Kuipers OP**. 2008. LysM, a widely distributed protein motif for
501 binding to (peptido)glycans. Mol Microbiol **68**:838–847.

502 23. **Rawlings ND**, **Barrett AJ**, **Thomas PD**, **Huang X**, **Bateman A**, **Finn RD**. 2018. The MEROPS
503 database of proteolytic enzymes, their substrates and inhibitors in 2017 and a comparison with
504 peptidases in the PANTHER database. Nucleic Acids Res **46**:D624–D632.

505 24. **O'Toole GA**, **Pratt LA**, **Watnick PI**, **Newman DK**, **Weaver VB**, **Kolter R**. 1999. Genetic
506 approaches to study of biofilms. Methods Enzymol **310**:91–109.

507 25. **Patzer SI**, **Hantke K**. 1998. The ZnuABC high-affinity zinc uptake system and its regulator Zur
508 in *Escherichia coli*. Mol Microbiol **28**:1199–1210.

509 26. **Gilston BA**, **Wang S**, **Marcus MD**, **Canalizo-Hernández MA**, **Swindell EP**, **Xue Y**,
510 **Mondragón A**, **O'Halloran TV**. 2014. Structural and Mechanistic Basis of Zinc Regulation

511 Across the *E. coli* Zur Regulon. PLoS Biol **12**:e1001987.

512 27. **Shin J-H**, **Helmann JD**. 2016. Molecular logic of the Zur-regulated zinc deprivation response in
513 *Bacillus subtilis*. Nat Commun **7**:1–9.

514 28. **Sheng Y**, **Fan F**, **Jensen O**, **Zhong Z**, **Kan B**, **Wang H**, **Zhu J**. 2015. Dual zinc transporter
515 systems in *Vibrio cholerae* promote competitive advantages over gut microbiome. Infect Immun
516 **83**:3902–3908.

517 29. **Panina EM**, **Mironov AA**, **Gelfand MS**. 2011. Comparative genomics of bacterial zinc
518 regulons: Enhanced ion transport, pathogenesis, and rearrangement of ribosomal proteins. Proc
519 Natl Acad Sci USA **100**:9912–9917.

520 30. **Novichkov PS**, **Kazakov AE**, **Ravcheev DA**, **Leyn SA**, **Kovaleva GY**, **Sutormin RA**, **Kazanov**
521 **MD**, **Riehl W**, **Arkin AP**, **Dubchak I**, **Rodionov DA**. 2013. RegPrecise 3.0 – A resource for
522 genome-scale exploration of transcriptional regulation in bacteria. BMC Genomics **14**:745.

523 31. **Crooks GE**, **Hon G**, **Chandonia J-M**, **Brenner SE**. 2004. WebLogo: a sequence logo generator.
524 Genome Res **14**:1188–1190.

525 32. **Napolitano M**, **Rubio MÁ**, **Camargo S**, **Luque I**. 2013. Regulation of internal promoters in a
526 zinc-responsive operon is influenced by transcription from upstream promoters. J Bacteriol
527 **195**:JB.01488–12–1293.

528 33. **Arslan P**, **Di Virgilio F**, **Beltrame M**, **Tsien RY**, **Pozzan T**. 1985. Cytosolic Ca2+ homeostasis
529 in Ehrlich and Yoshida carcinomas. A new, membrane-permeant chelator of heavy metals reveals
530 that these ascites tumor cell lines have normal cytosolic free Ca^{2+}. J Biol Chem **260**:2719–2727.

531 34. **Yamamoto H**, **Kurosawa S-I**, **Sekiguchi J**. 2003. Localization of the vegetative cell wall

532 hydrolases LytC, LytE, and LytF on the *Bacillus subtilis* cell surface and stability of these
533 enzymes to cell wall-bound or extracellular proteases. J Bacteriol **185**:6666–6677.

534 35. **Altschul SF**, **Gish W**, **Miller W**, **Myers EW**, **Lipman DJ**. 1990. Basic local alignment search
535 tool. J Mol Biol **215**:403–410.

536 36. **Li Y**, **Qiu Y**, **Gao H**, **Guo Z**, **Han Y**, **Song Y**, **Du Z**, **Wang X**, **Zhou D**, **Yang R**. 2009.
537 Characterization of Zur-dependent genes and direct Zur targets in *Yersinia pestis*. BMC Microbiol
538 **9**:128.

539 37. **Mortensen BL**, **Rathi S**, **Chazin WJ**, **Skaar EP**. 2014. *Acinetobacter baumannii* response to
540 host-mediated zinc limitation requires the transcriptional regulator Zur. J Bacteriol
541 **196**:JB.01650–14–2626.

542 38. **Maciąg A**, **Dainese E**, **Rodriguez GM**, **Milano A**, **Provvedi R**, **Pasca MR**, **Smith I**, **Palù G**,
543 **Riccardi G**, **Manganelli R**. 2007. Global analysis of the *Mycobacterium tuberculosis* Zur (FurB)
544 regulon. J Bacteriol **189**:730–740.

545 39. **Pawlik M-C**, **Hubert K**, **Joseph B**, **Claus H**, **Schoen C**, **Vogel U**. 2012. The zinc-responsive
546 regulon of *Neisseria meningitidis* comprises seventeen genes under control of a Zur element. J
547 Bacteriol **194**:JB.01091–12–6603.

548 40. **Mazzon RR**, **Braz VS**, **da Silva Neto JF**, **do Valle Marques M**. 2014. Analysis of the
549 *Caulobacter crescentus* Zur regulon reveals novel insights in zinc acquisition by TonB-dependent
550 outer membrane proteins. BMC Genomics **15**:734.

551 41. **Gaballa A**, **Wang T**, **Ye RW**, **Helmann JD**. 2002. Functional analysis of the *Bacillus subtilis*
552 Zur regulon. J Bacteriol **184**:6508–6514.

553 42. **Schröder J**, **Jochmann N**, **Rodionov DA**, **Tauch A**. 2010. The Zur regulon of *Corynebacterium*
554 *glutamicum* ATCC 13032. BMC Genomics **11**:12.

555 43. **Kallifidas D**, **Pascoe B**, **Owen GA**, **Strain-Damerell CM**, **Hong H-J**, **Paget MSB**. 2010. The
556 zinc-responsive regulator Zur controls expression of the coelibactin gene cluster in *Streptomyces*
557 *coelicolor*. J Bacteriol **192**:608–611.

558 44. **Sigdel TK**, **Easton JA**, **Crowder MW**. 2006. Transcriptional response of *Escherichia coli* to
559 TPEN. J Bacteriol **188**:6709–6713.

560 45. **Hensley MP**, **Gunasekera TS**, **Easton JA**, **Sigdel TK**, **Sugarbaker SA**, **Klingbeil L**, **Breece**
561 **RM**, **Tierney DL**, **Crowder MW**. 2012. Characterization of Zn(II)-responsive ribosomal
562 proteins YkgM and L31 in *E. coli*. J Inorg Biochem **111**:164–172.

563 46. **Fukushima T**, **Afkham A**, **Kurosawa S-I**, **Tanabe T**, **Yamamoto H**, **Sekiguchi J**. 2006. A New
564 d,l-endopeptidase gene product, YojL (renamed CwlS), plays a role in cell separation with LytE
565 and LytF in *Bacillus subtilis*. J Bacteriol **188**:5541–5550.

566 47. **Smith TJ**, **Blackman SA**, **Foster SJ**. 2000. Autolysins of *Bacillus subtilis*: multiple enzymes
567 with multiple functions. Microbiology **146**:249–262.

568 48. **Takahashi H**, **Oshima T**, **Hobman JL**, **Doherty N**, **Clayton SR**, **Iqbal M**, **Hill PJ**, **Tobe T**,
569 **Ogasawara N**, **Kanaya S**, **Stekel DJ**. 2015. The dynamic balance of import and export of zinc in
570 *Escherichia coli* suggests a heterogeneous population response to stress. J R Soc Interface
571 **12**:20150069–20150069.

572 49. **Ragumani S**, **Kumaran D**, **Burley SK**, **Swaminathan S**. 2008. Crystal structure of a putative
573 lysostaphin peptidase from Vibrio cholerae. Proteins: Struct, Funct, Bioinf **72**:1096–1103.

574 50. **Kehl-Fie TE**, **Skaar EP**. 2010. Nutritional immunity beyond iron: a role for manganese and zinc.
575 Current Opinion in Chemical Biology **14**:218–224.

576 51. **Ma L**, **Terwilliger A**, **Maresso AW**. 2015. Iron and zinc exploitation during bacterial
577 pathogenesis. Metallomics **7**:1541–1554.

578 52. **Hood MI**, **Mortensen BL**, **Moore JL**, **Zhang Y**, **Kehl-Fie TE**, **Sugitani N**, **Chazin WJ**,
579 **Caprioli RM**, **Skaar EP**. 2012. Identification of an *Acinetobacter baumannii* zinc acquisition
580 system that facilitates resistance to calprotectin-mediated zinc sequestration. PLoS Pathog
581 **8**:e1003068.

582 53. **Sabri M**, **Houle S**, **Dozois CM**. 2009. Roles of the extraintestinal pathogenic *Escherichia coli*
583 ZnuACB and ZupT Zinc transporters during urinary tract infection. Infect Immun **77**:1155–1164.

584 54. **Gabbianelli R**, **Scotti R**, **Ammendola S**, **Petrarca P**, **Nicolini L**, **Battistoni A**. 2011. Role of
585 ZnuABC and ZinT in *Escherichia coli* O157:H7 zinc acquisition and interaction with epithelial
586 cells. BMC Microbiol **11**:36.

587 55. **Ammendola S**, **Pasquali P**, **Pistoia C**, **Petrucci P**, **Petrarca P**, **Rotilio G**, **Battistoni A**. 2007.
588 High-affinity Zn^{2+} uptake system ZnuABC is required for bacterial zinc homeostasis in
589 intracellular environments and contributes to the virulence of *Salmonella enterica*. Infect Immun
590 **75**:5867–5876.

591 56. **Cerasi M**, **Ammendola S**, **Battistoni A**. 2013. Competition for zinc binding in the host-pathogen
592 interaction. Front Cell Infect Microbiol **3**.

593 57. **O'Shea YA**, **Reen FJ**, **Quirke AM**, **Boyd EF**. 2004. Evolutionary genetic analysis of the
594 emergence of epidemic *Vibrio cholerae* isolates on the basis of comparative nucleotide sequence
595 analysis and multilocus virulence gene profiles. J Clin Microbiol **42**:4657–4671.

596 58. **Hu D**, **Liu B**, **Feng L**, **Ding P**, **Guo X**, **Wang M**, **Cao B**, **Reeves PR**, **Wang L**. 2016. Origins of
597 the current seventh cholera pandemic. Proc Natl Acad Sci USA **113**:E7730–E7739.

598 59. **Gibson DG**, **Young L**, **Chuang R-Y**, **Venter JC**, **Hutchison CA III**, **Smith HO**. 2009.
599 Enzymatic assembly of DNA molecules up to several hundred kilobases. Nat Methods **6**:343–
600 345.

601 60. **Donnenberg MS**, **Kaper JB**. 1991. Construction of an eae deletion mutant of enteropathogenic
602 *Escherichia coli* by using a positive-selection suicide vector. Infect Immun **59**:4310–4317.

603 61. **Butterton JR**, **Beattie DT**, **Gardel CL**, **Carroll PA**, **Hyman T**, **Killeen KP**, **Mekalanos JJ**,
604 **Calderwood SB**. 1995. Heterologous antigen expression in *Vibrio cholerae* vector strains. Infect
605 Immun **63**:2689–2696.

606 62. **Chiang SL**, **Rubin EJ**. 2002. Construction of a mariner-based transposon for epitope-tagging and
607 genomic targeting. Gene **296**:179–185.

608 63. **Alvarez L**, **Hernandez SB**, **de Pedro MA**, **Cava F**. 2016. Ultra-sensitive, high-resolution liquid
609 chromatography methods for the high-throughput quantitative analysis of bacterial cell wall
610 chemistry and structure. pp. 11–27. *In* Bacterial Cell Wall Homeostasis. Humana Press, New
611 York, NY, New York, NY.

612 64. **Paintdakhi A**, **Parry B**, **Campos M**, **Irnov I**, **Elf J**, **Surovtsev I**, **Wagner CJ**. 2016. Oufti: an
613 integrated software package for high-accuracy, high-throughput quantitative microscopy analysis.
614 Mol Microbiol **99**:767–777.

615 65. **Apweiler R**, **Bairoch A**, **Wu CH**, **Barker WC**, **Boeckmann B**, **Ferro S**, **Gasteiger E**, **Huang**
616 **H**, **Lopez R**, **Magrane M**, **Martin MJ**, **Natale DA**, **O'Donovan C**, **Redaschi N**, **Yeh LSL**.
617 2004. UniProt: the universal protein knowledgebase. Nucleic Acids Res **32**:D115–D119.

618 66. **Fong C**, **Rohmer L**, **Radey M**, **Wasnick M**, **Brittnacher MJ**. 2008. PSAT: A web tool to
619 compare genomic neighborhoods of multiple prokaryotic genomes. BMC Bioinformatics **9**:170.

620

621 **Figure Legends**

622 **Fig 1. *shyB* is a LysM/M23 endopeptidase that is transcribed in minimal medium.**

623 **(A)** Model of the peptidoglycan sacculus indicating EP cleavage sites **(B)** The *V. cholerae* genome
624 encodes three endopeptidases (ShyA, ShyB, ShyC) possessing a hydrophobic region (gray), a PG
625 binding domain (LysM, pink), and metallo-endopeptidase domain (M23, green). Protein domains were
626 annotated using UniProt (65). **(C)** *lacZ* transcriptional reporters for each endopeptidase spotted onto LB
627 (top row) and M9 minimal (bottom row) agar containing X-gal. A blue colony color indicates that the
628 promoter is actively transcribed. Wild-type (WT) and Δ*lacZ* strain are included as positive and negative
629 controls, respectively.

630

631 **Fig 2. *shyB* transcription is regulated by zinc homeostasis.**

632 **(A)** The *shyB* transcriptional reporter (*lacZ::*P_{shyB}*:lacZ*) was mutagenized with a Himar1 mariner
633 transposon and screened for *shyB* induction (blue colonies) on LB agar containing X-gal and selective
634 antibiotics (see Methods). Representative dark blue (black arrow) and light blue (white arrows) colonies
635 are shown. Approximate Tn insertion sites identified by arbitrary PCR are shown (triangles). **(B)** The
636 *shyB* transcriptional reporter in a wild-type, Δ*zur*, or Δ*znuABC* background were grown on M9 X-gal
637 agar without (top row) or with (bottom row) 10 μM $ZnSO_4$.

638

639 **Fig 3. Zur directly binds the *shyB* promoter.**

640 **(A)** The *shyB* promoter, annotated with a 5'-RACE transcription start site (+1) and putative -10 region
641 (box), was aligned with a *Vibrio* Zur sequence logo (30, 31). The inverted AT-rich repeat in the putative

642 Zur-box is underlined with black arrows**. (B)** A chemiluminescent probe containing the putative *shyB*
643 Zur box was incubated with purified Zur in the presence of $ZnCl_2$ (5 μM). Zur binding specificity was
644 tested by adding 100-fold molar excess of unlabeled specific (S, Lane 3) or non-specific (NS, Lane 4)
645 competitor DNA. Samples were electrophoresed on a 6% DNA retardation gel to separate unbound
646 (black arrow) and bound probe (white arrow).
647

648 **Fig 4**. ***shyB* supports cell growth in chelated medium and is conditionally essential in a Δ*shyA***
649 **mutant.**

650 Mid-exponential cultures of the indicated *V. cholerae* mutants were washed to remove IPTG before
651 being diluted 1:100 into M9 glucose containing streptomycin plus TPEN (250 nM) in the absence (A,C)
652 or presence (B,D) of $ZnSO_4$ (1 μM). Growth of each strain was monitored by optical density (OD600) in
653 a Bioscreen C 100-well plate. Error bars report standard error of the mean (SEM) for three independent
654 biological replicates. **(A-B)** Log-transformed growth curves are shown for WT (green circle), Δ*shyAC*
655 *lacZ::*P_{tac}*:shyA* (blue square), and Δ*shyABC lacZ::*P_{tac}*:shyA* (red triangle). **(C-D)** In a similar growth
656 experiment, growth rates of WT (solid black), single mutants (solid gray) and double mutants (striped)
657 were calculated from exponential phase and normalized to the average WT growth rate (%). Statistical
658 difference relative to WT was assessed using two-way analysis of variance (ANOVA) followed by
659 Dunnett's multiple comparison test (***, p-value < 0.001).
660

661 **Fig 5. ShyB retains endopeptidase activity in EDTA.**

662 *V. cholerae* sacculi was digested with 10 μg of purified ShyA, ShyB, or ShyC for 16 h at 37°C in the
663 absence **(A)** or presence **(C)** of 1mM EDTA. The soluble products released by digested sacculi were
664 separated by size via HPLC and quantified by absorbance (204 nm). (**B, D**) The remaining insoluble
665 pellet was digested with muramidase and soluble products were separated by HPLC.
666

667 **Fig 6. ShyBmsfGFP localizes to the midcell during division.**

668 *V. cholerae* expressing a C-terminal fluorescent fusion (*lacZ::*P_{tac}*-shyBmsfGFP*) was grown overnight in
669 M9 + IPTG (200 μM). (A) The ShyBmsfGFP fusion was imaged on an agarose patch (0.8% agarose in
670 M9 minimal medium) with 300 ms exposure at 490 nm. (B) A heat map showing intensity of fluorescent
671 signal as a function of distance from the midcell ("demograph") was generated from over 1,800 cells in
672 Oufti (64).

673

674 **Fig 7. ShyB/MepM homologs are adjacent to the Zur-controlled *znu* operon in many Gram-**
675 **negative pathogens.**

676 Gene neighborhood alignments generated by Prokaryotic Sequence Homology Analysis Tool (PSAT)
677 from 7 different Gram-negative bacteria (66). Arrows indicate the approximate location of the
678 bidirectional promoter and site of Zur-binding in the *znu* operon. Asterisks indicate that co-transcription
679 of *znu* and the downstream M23 endopeptidase is supported by transcriptomic data.

680

681 **Fig S1. Δ*zur* and Δ*znuABC* deletions induce the *shyB* promoter on LB agar.**

682 Clean deletions of Δ*zur* and Δ*znuA* in the P_{shyB}*:lacZ* transcriptional reporter were complemented with an
683 arabinose-inducible (pBAD) plasmid carrying the respective gene *in trans*. Strains were plated onto LB
684 agar containing x-gal (40 μg mL^{-1}), chloramphenicol (10 μg mL^{-1}), and arabinose (0.2%). Plates were
685 incubated overnight and then at room temperature for 2 days.

686

687 **Fig S2. *shyB* promoter is repressed by exogenous zinc, but not by other transition metals.**

688 The P_{shyB}*:lacZ* transcriptional reporter was plated on M9 X-gal agar containing 10 μM of $ZnSO_4$, $FeSO_4$,
689 or $MnCl_2$. Plates were incubated overnight and then at room temperature for 2 days.

690

691 **Fig S3. Western Blot of ShyB and ShyC protein levels in high and low-zinc media.**

692 N16961 strains encoding ShyB ΔlysM::6His-FLAG or ShyC:6His-FLAG were grown in M9 glucose
693 (0.4%) with added TPEN (250 nM) or TPEN plus ZnSO4 (1 μM). Cells were harvested at mid-log
694 (OD600 = 0.4) and lysed via SDS boiling and sonication. Western blot was performed using standard
695 techniques. Blots were developed using a mouse anti-FLAG F1804 primary antibody (Sigma Aldrich)
696 and Goat anti-Mouse IR CW800 secondary antibody (LI-COR Biosciences). Blots were imaged using a
697 Lycor Odyssey CLx imager.
698

699 **Fig S4. EDTA-induced *shyB* expression restores growth to Δ*shyAC*.**

700 Wt (green), Δ*shyAC lacZ::*P_{tac}*-shyA* (blue), and Δ*shyABC lacZ::*P_{tac}*-shyA* (red) strains were grown in
701 M9 glucose (0.4%) containing **(A)** EDTA (30 μM) (solid lines) or **(B)** EDTA plus $ZnSO_4$ (60 μM)
702 (dashed lines). Growth of each 200 μL culture was measured by optical density (600 nm) in a Bioscreen
703 C 100-well plate. Error bars report standard error of the mean (SEM) for three biologically independent
704 replicates.
705

706 **Fig S5. *zur* deletion restores growth to Δ*shyAC* in LB medium.**

707 Overnight cultures (grown in LB/streptomycin at 37°C) were subcultured 1:100 into fresh media and
708 grown at 37°C until mid-log phase. Δ*zur lacZ::*P_{tac}*-zur* (blue) and Δ*zur* Δ*shyAC lacZ::*P_{tac}*-zur* (red) were
709 diluted 1:100 into LB (solid lines) or in LB plus IPTG (200 μM) (dashed lines). Growth of each strain
710 was monitored by optical density (OD600) in a Bioscreen C 100-well plate. Error bars report standard
711 error of the mean (SEM) for three biologically independent replicates.
712

713 **Fig S6. Inducible *shyB* expression rescues growth of Δ*shyABC*.**

714 Strains were grown overnight in LB/streptomycin plus IPTG (200uM) at 37°C. Cells were washed,
715 subcultured 1:10 into M9 glucose (0.4%), and grown at 37°C for 2 hours. Wt (dotted lines) and
716 Δ*shyABC lacZ::*P_{tac}*-shyA* vc1807*::*P_{ara}*-shyB* (solid lines) strains were diluted 1:100 in M9 glucose

717 (0.4%) (orange), with 200 μM IPTG (green) or with 0.2% arabinose (black). Growth of each 200 μL
718 culture was measured by optical density (600 nm) in a Bioscreen C 100-well plate. Error bars report
719 standard error of the mean (SEM) for three biologically independent replicates.
720
721 **Fig S7. A point mutation in the ShyB active site abolishes endopeptidase activity *in vitro*.**
722 Purified ShyB, and ShyB H370A were incubated with purified *V. cholerae* sacculi for 16 h at 37°C. **(A)**
723 The soluble products released by digested were separated by HPLC and quantified by absorbance (204
724 nm). **(B)** The remaining pellet was digested with muramidase and the soluble products were separated
725 by HPLC and quantified by absorbance.
726
727 **Fig S8. Sequential digestion of *V. cholerae* sacculi by Shy endopeptidases.**
728 10 μg of purified (**A**) ShyA, (**B**) ShyB, and (**C**) ShyC were incubated with *V. cholerae* sacculi for 16 h at
729 37°C, followed by secondary digestion a different endopeptidase. The soluble products released by
730 digested sacculi were separated by size via HPLC and quantified by absorbance (204 nm).
731
732 **Fig S9. ShyBmsfGFP translational fusion rescues growth of Δ*shyAB* in TPEN-chelated medium.**
733 Mid-exponential cultures of WT (blue), Δ*shyAB* (red), Δ*shyAB lacZ::P$_{tac}$-shyB* (green), and Δ*shyAB*
734 *lacZ::P$_{tac}$-shyB* (orange, purple) were washed and subcultured 1:100 into M9 containing TPEN (250
735 nM) with and without IPTG (200 μM). Growth of each culture at 37°C was measured by optical density
736 (600 nm). Error bars report standard error of the mean (SEM) for three biologically independent
737 replicates.
738
739 **Table S1. Summary of ShyB homologs that contain an upstream, canonical Zur box.**
740
741 **Table S2. Summary of oligonucleotides used in this study.**

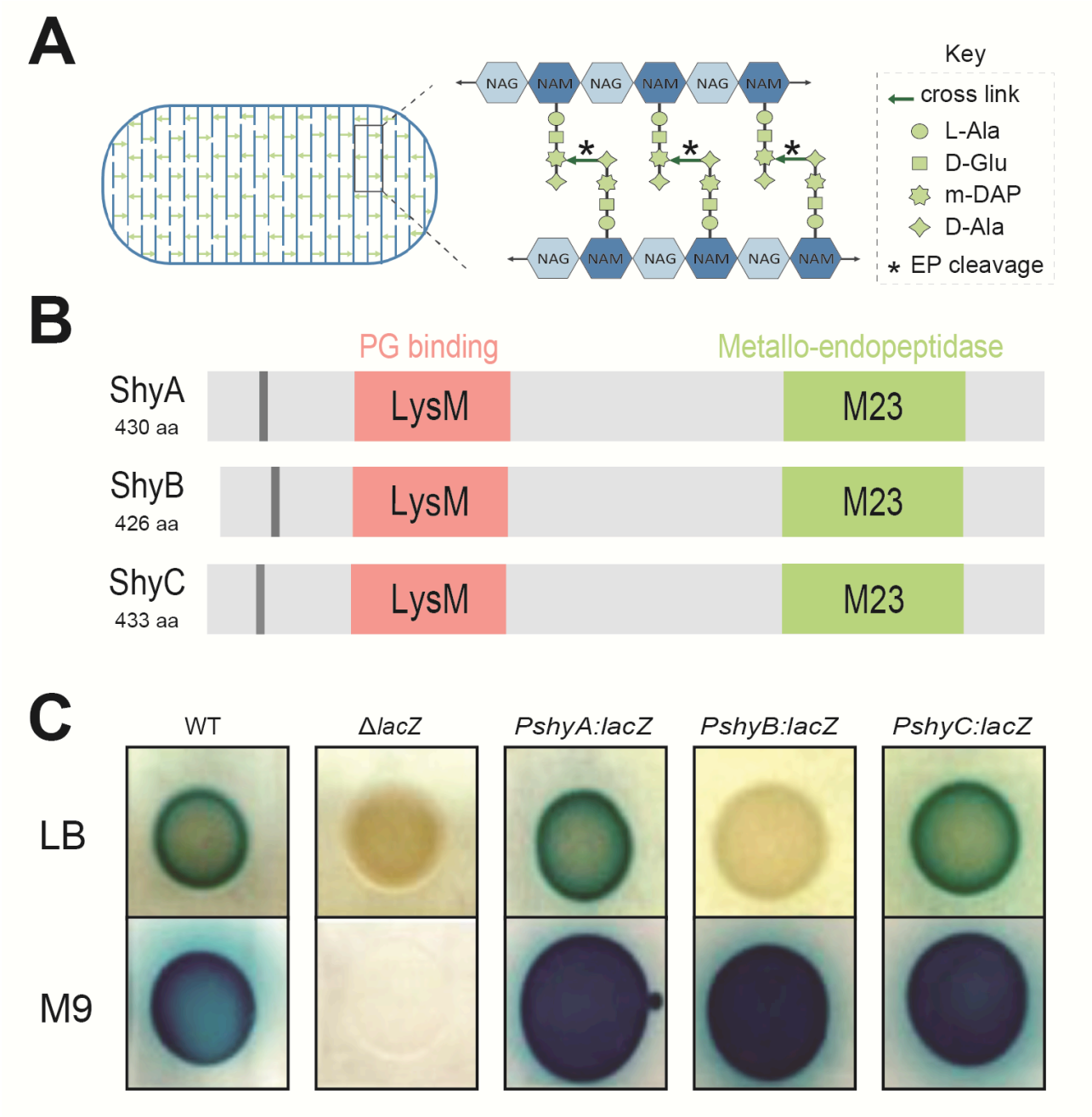

Fig 1. *shyB* is a LysM/M23 endopeptidase that is transcribed in minimal medium.

(A) Model of the peptidoglycan sacculus indicating EP cleavage sites **(B)** The *V. cholerae* genome encodes three endopeptidases (ShyA, ShyB, ShyC) possessing a hydrophobic region (gray), a PG binding domain (LysM, pink), and metallo-endopeptidase domain (M23, green). Protein domains were annotated using UniProt (1). **(C)** *lacZ* transcriptional reporters for each endopeptidase spotted onto LB (top row) and M9 minimal (bottom row) agar containing X-gal. A blue colony color indicates that the promoter is actively transcribed. Wild-type (WT) and Δ*lacZ* strain are included as positive and negative controls, respectively.

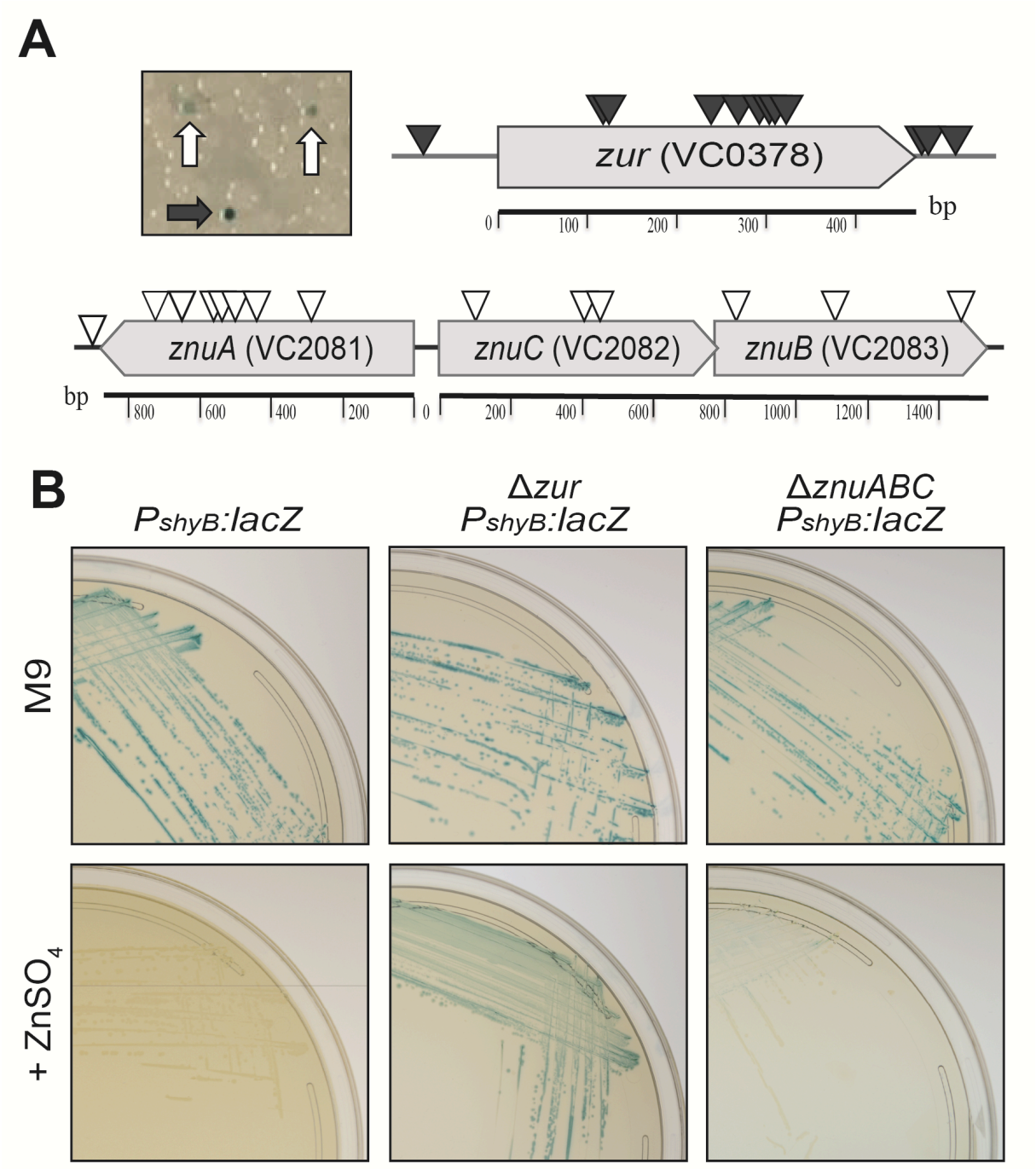

Fig 2. *shyB* transcription is regulated by zinc homeostasis.

(A) The *shyB* transcriptional reporter (*lacZ::*P_{shyB}*:lacZ*) was mutagenized with a Himar1 mariner transposon and screened for *shyB* induction (blue colonies) on LB agar containing X-gal and selective antibiotics (see Methods). Representative dark blue (black arrow) and light blue (white arrows) colonies are shown. Approximate Tn insertion sites identified by arbitrary PCR are shown (triangles). **(B)** The *shyB* transcriptional reporter in a wild-type, Δ*zur*, or Δ*znuABC* background were grown on M9 X-gal agar without (top row) or with (bottom row) 10 μM $ZnSO_4$.

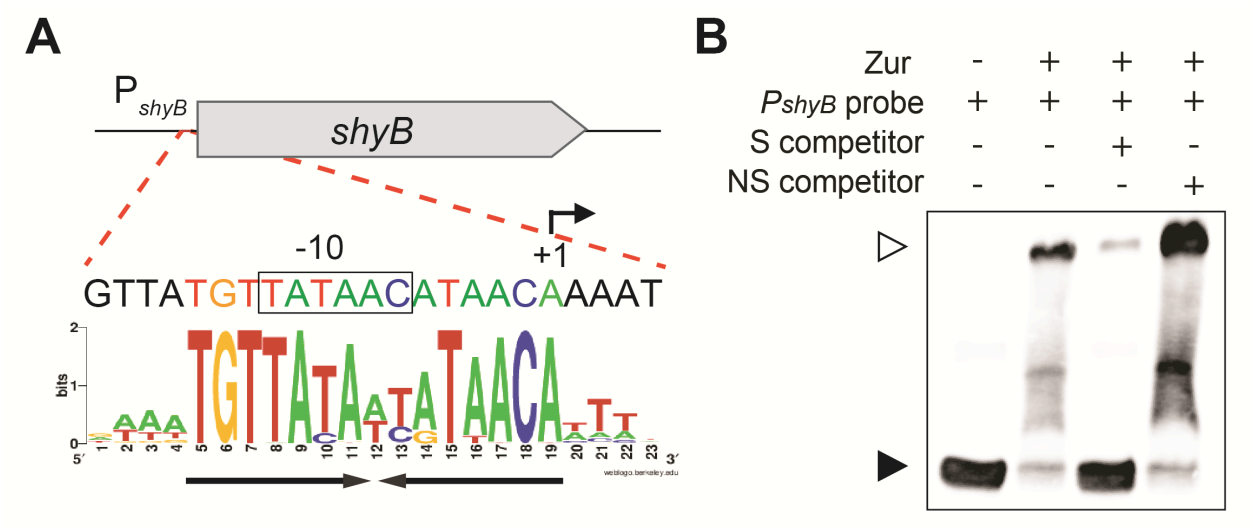

Fig 3. Zur directly binds the *shyB* promoter.

(A) The *shyB* promoter, annotated with a 5'-RACE transcription start site (+1) and putative -10 region (box), was aligned with a *Vibrio* Zur sequence logo (30, 31). The inverted AT-rich repeat in the putative Zur-box is underlined with black arrows**. (B)** A chemiluminescent probe containing the putative *shyB* Zur box was incubated with purified Zur in the presence of $ZnCl_2$ (5 µM). Zur binding specificity was tested by adding 100-fold molar excess of unlabeled specific (S, Lane 3) or non-specific (NS, Lane 4) competitor DNA. Samples were electrophoresed on a 6% DNA retardation gel to separate unbound (black arrow) and bound probe (white arrow).

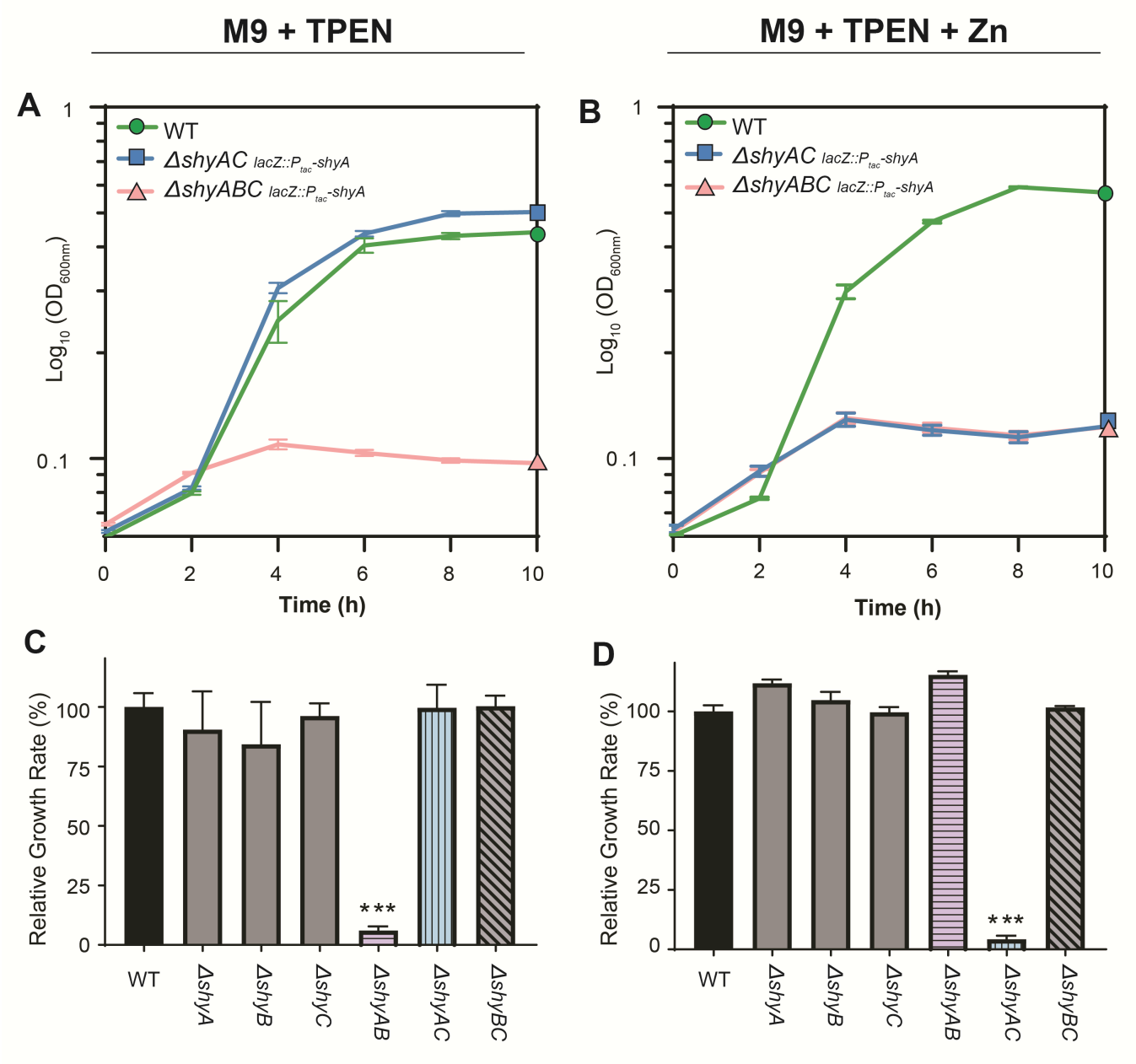

Fig 4. ***shyB* supports cell growth in chelated medium and is conditionally essential in a Δ*shyA* mutant.**

Mid-exponential cultures of the indicated *V. cholerae* mutants were washed to remove IPTG before being diluted 1:100 into M9 glucose containing streptomycin plus TPEN (250 nM) in the absence (A,C) or presence (B,D) of $ZnSO_4$ (1 μM). Growth of each strain was monitored by optical density (OD600) in a Bioscreen C 100-well plate. Error bars report standard error of the mean (SEM) for three independent biological replicates. **(A-B)** Log-transformed growth curves are shown for WT (green circle), Δ*shyAC lacZ::P*$_{tac}$*:shyA* (blue square), and Δ*shyABC lacZ::P*$_{tac}$*:shyA* (red triangle). **(C-D)** In a similar growth experiment, growth rates of WT (solid black), single mutants (solid gray) and double mutants (striped) were calculated from exponential phase and normalized to the average WT growth rate (%). Statistical difference relative to WT was assessed using two-way analysis of variance (ANOVA) followed by Dunnett's multiple comparison test (***, p-value < 0.001).

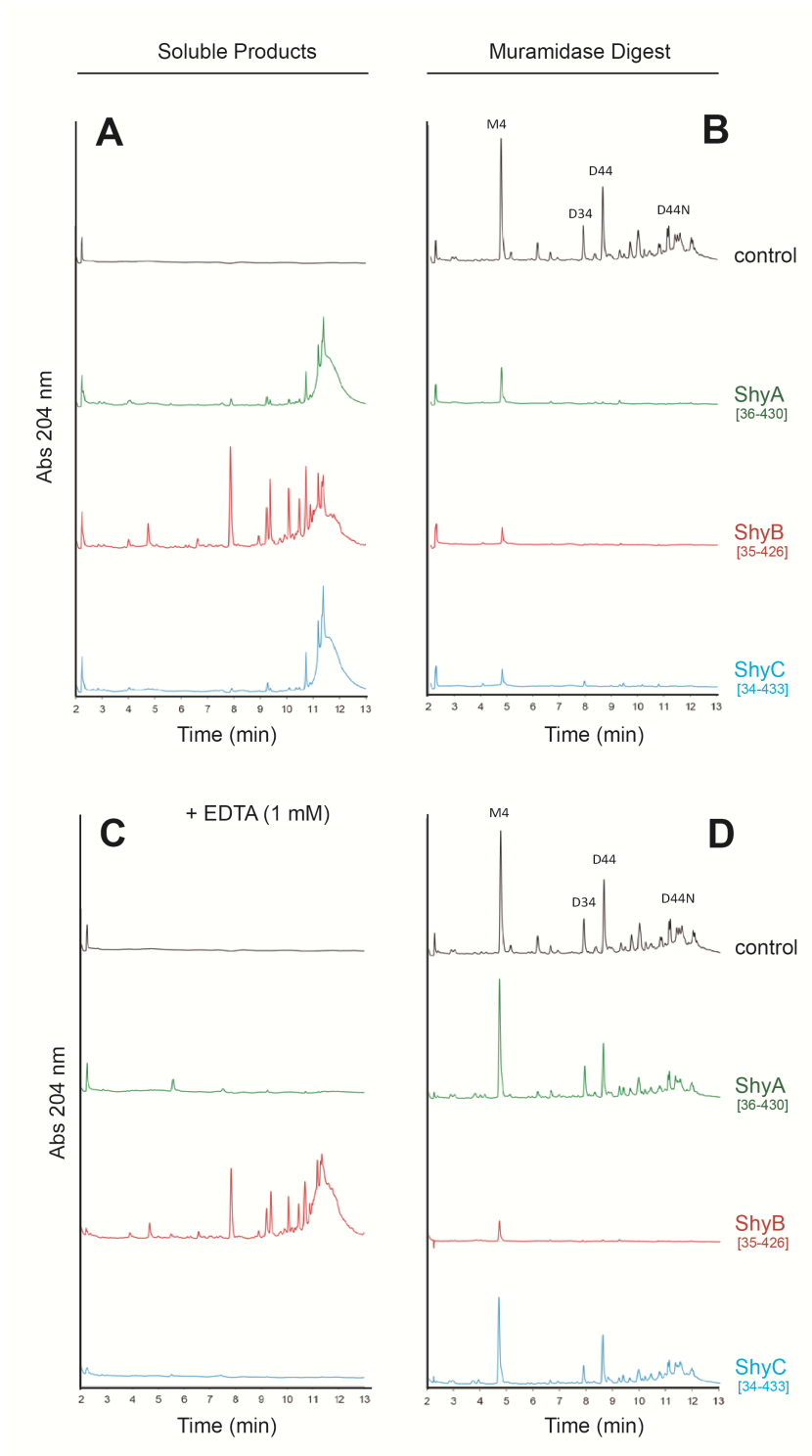

Fig 5. ShyB retains endopeptidase activity in EDTA.

V. cholerae sacculi was digested with 10 µg of purified ShyA, ShyB, or ShyC for 16 h at 37°C in the absence **(A)** or presence **(C)** of 1mM EDTA. The soluble products released by digested sacculi were separated by size via HPLC and quantified by absorbance (204 nm). (**B, D**) The remaining insoluble pellet was digested with muramidase and soluble products were separated by HPLC.

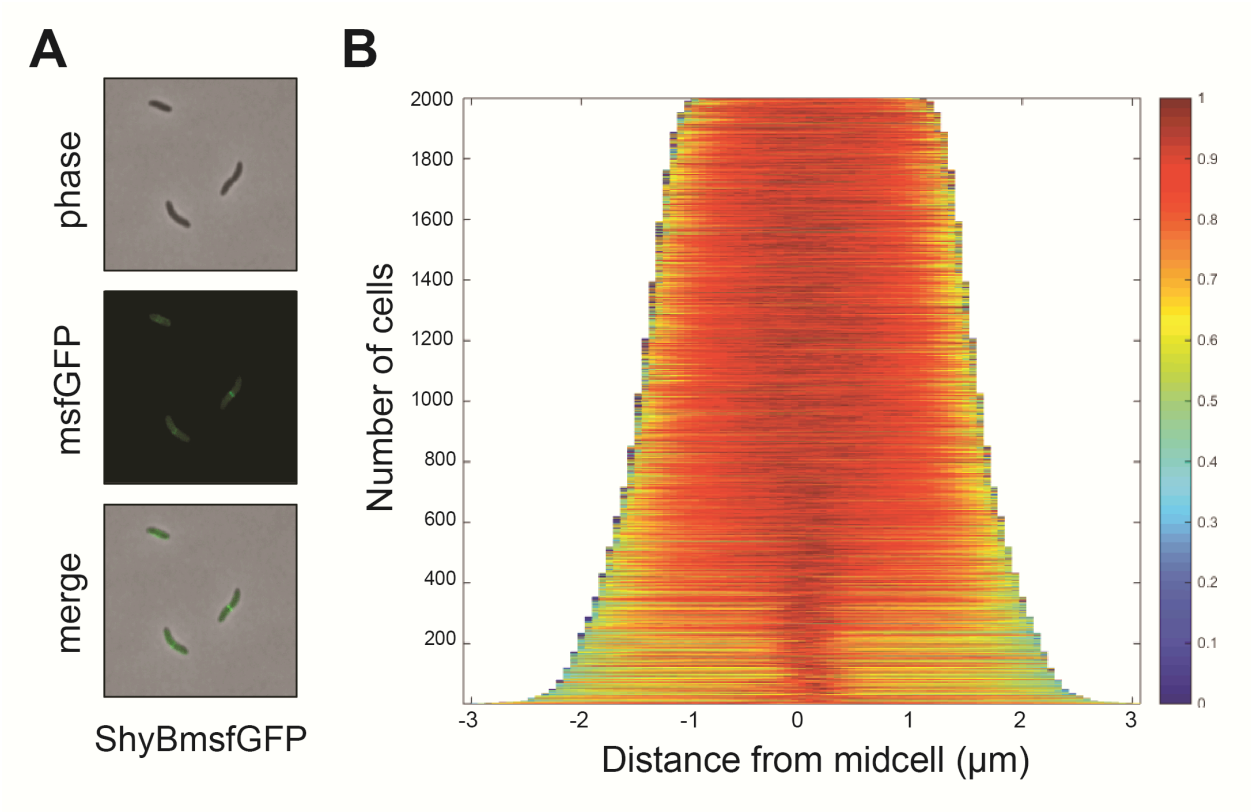

Fig 6. ShyBmsfGFP localizes to the midcell during division.

V. cholerae expressing a C-terminal fluorescent fusion (*lacZ::*P_{tac}*-shyBmsfGFP*) was grown overnight in M9 + IPTG (200 μM). (A) The ShyBmsfGFP fusion was imaged on an agarose patch (0.8% agarose in M9 minimal medium) with 300 ms exposure at 490 nm. (B) A heat map showing intensity of fluorescent signal as a function of distance from the midcell ("demograph") was generated from over 1,800 cells in Oufti (64).

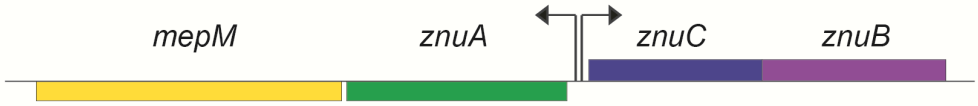

Escherichia coli K12 MG1655	*	b1856	b1857	b1858	b1859
Escherichia coli 0157:H7		Z2908	Z2909	Z2910	Z2911
Escherichia coli O127:H6		E2348C_1981	E2348C_1982	E2348C_1983	E2348C_1984
Yersinia pestis CO92	*	YPO2062	YPO2061	YPO2060	YPO2059
Salmonella typhimurium LT2		STM1890	STM1891	STM1892	STM1893
Enterobacter cloacae ATCC 13047		ECL_01442	ECL_01441	ECL_01440	ECL_01439
Klebsiella pneumoniae 342		KPK_1913	KPK_1912	KPK_1911	KPK_1910

Fig 7. ShyB/MepM homologs are adjacent to the Zur-controlled *znu* operon in many Gram-negative pathogens.

Gene neighborhood alignments generated by Prokaryotic Sequence Homology Analysis Tool (PSAT) from 7 different Gram-negative bacteria (66). Arrows indicate the approximate location of the bidirectional promoter and site of Zur-binding in the *znu* operon. Asterisks indicate that co-transcription of *znu* and the downstream M23 endopeptidase is supported by transcriptomic data.